Title

Blockade of current through single calcium channels by Cd2+, Mg2+, and Ca2+. Voltage and concentration dependence of calcium entry into the pore.

Journal

The Journal of general physiology, 88(3)

ISSN

0022-1295

Authors

Lansman, JB
Hess, P
Tsien, RW

Publication Date

1986-09-01

DOI

10.1085/jgp.88.3.321

Peer reviewed

Blockade of Current through Single Calcium Channels by Cd^{2+}, Mg^{2+}, and Ca^{2+}

Voltage and Concentration Dependence of Calcium Entry into the Pore

JEFFRY B. LANSMAN, PETER HESS, and RICHARD W. TSIEN

From the Department of Physiology, Yale University School of Medicine, New Haven, Connecticut 06511

ABSTRACT We studied the blocking actions of external Ca^{2+}, Mg^{2+}, Ca^{2+}, and other multivalent ions on single Ca channel currents in cell-attached patch recordings from guinea pig ventricular cells. External Cd or Mg ions chopped long-lasting unitary Ba currents promoted by the Ca agonist Bay K 8644 into bursts of brief openings. The bursts appear to arise from discrete blocking and unblocking transitions. A simple reaction between a blocking ion and an open channel was suggested by the kinetics of the bursts: open and closed times within a burst were exponentially distributed, the blocking rate varied linearly with the concentration of blocking ion, and the unblocking rate was more or less independent of the blocker concentration. Other kinetic features suggested that both Cd^{2+} and Mg^{2+} lodge within the pore. The unblocking rate was speeded by membrane hyperpolarization or by raising the Ba concentration, as if blocking ions were swept into the myoplasm by the applied electric field or by repulsive interaction with Ba^{2+}. Ca ions reduced the amplitude of unitary Ba currents (50% inhibition at ~10 mM $[Ca]_o$ with 50 mM $[Ba]_o$) without detectable flicker, presumably because Ca ions exit the pore very rapidly following Ba entry. However, Ca^{2+} entry and exit rates could be resolved when micromolar Ca blocked unitary Li^+ fluxes through the Ca channel. The blocking rate was essentially voltage independent, but varied linearly with Ca concentration (rate coefficient, 4.5×10^8 $M^{-1}s^{-1}$); evidently, the initial Ca^{2+}-pore interaction is outside the membrane field and much faster than the overall process of Ca ion transfer. The unblocking rate did not vary with $[Ca]_o$, but increased steeply with membrane hyperpolarization, as if blocking Ca ions were driven into the cell. We suggest that Ca is both an effective permeator and a potent blocker because it dehydrates rapidly (unlike Mg^{2+}) and binds to the pore with appropriate affinity (unlike Cd^{2+}). There appears to be no sharp dichotomy

Address reprint requests to Dr. Peter Hess, Dept. of Physiology and Biophysics, Harvard University, 25 Shattuck St., Boston, MA 02115. Dr. Lansman's present address is Dept. of Pharmacology, University of California at San Francisco, 520 Parnassus Ave., San Francisco, CA 94143.

J. GEN. PHYSIOL. © The Rockefeller University Press · 0022-1295/86/09/0321/27 $1.00

Volume 88 September 1986 321–347

between "permeators" and "blockers," only quantitative differences in how quickly ions enter and leave the pore.

INTRODUCTION

It is well known that Ca currents through Ca channels can be blocked by a wide variety of multivalent cations including Mg^{2+}, Mn^{2+}, Co^{2+}, Cd^{2+}, and La^{3+} (Hagiwara and Byerly, 1981; Edwards, 1982), but there is no general agreement about the inhibitory mechanism(s). The proposals include: (*a*) a reduction of the local Ca concentration through screening of negative surface charge (Muller and Finkelstein, 1974), (*b*) competition with permeant ions for a site within the pore itself (Hagiwara et al., 1974), and (*c*) an additional action through regulatory sites outside the channel (Kostyuk et al., 1983). While studies of Ca channel block have so far relied largely on recordings from large numbers of channels, it is clear that these hypotheses can be tested most easily at the level of single channels. Such is the approach in this article.

Using the same experimental system as in the previous article (Hess et al., 1986), we were able to observe discrete interruptions of unitary Ca channel current with several blocking ions, including Ca^{2+} itself. The resolution of individual steps of block and unblock is new for Ca channels, although it follows valuable precedents in the study of monovalent cation channels (e.g., Armstrong, 1975; Neher and Steinbach, 1978; Fukushima, 1982; Yellen, 1984). The kinetics of block and unblock varied with blocker concentration, permeant ion concentration, and membrane potential, in a pattern consistent with the idea that blocking ions lodge within the pore, partway along the path of permeation. Apparently, block is an expression of the same fundamental ion-pore interactions that help govern ion permeation. The results for Ca^{2+} provide fundamental information about the rates of its entry and exit, and a comparison of Ca^{2+} with other ions leads to suggestions about the basis for Ca channel selectivity.

METHODS

The methods for isolating single ventricular cells and recording from cell-attached membrane patches are described in the preceding article (Hess et al., 1986). Voltage steps were applied to the patch pipette at a rate of 0.33 Hz. Current records were filtered at 1 kHz, sampled at 5 kHz, and stored on the hard disk of a PDP 11/23 computer.

The vast majority of the experiments were carried out in the presence of Bay K 8644 with the rationale of reducing interference from intrinsic channel closings caused by gating (see Hess et al., 1986, for references). The Ca channel agonist promotes a pattern of Ca channel gating ("mode 2") with characteristically long-lasting channel openings, and thereby allows clear expression of blocking events as bursts of brief openings (see Fig. 1). Two observations support the assumption that the bursts do not arise from rapid binding and unbinding of Bay K 8644. (*a*) Variations in the concentration of Bay K 8644 between 1 and 5 μM had no detectable effect on the kinetics of block. (*b*) Blocking ions reduced the mean open time of Ca channels even in the absence of Bay K 8644. As might be expected, high concentrations of blocker are required to make the blocking rate rapid enough to be distinguished from a background of rapid channel closings in the absence of Ca agonist.

To analyze bursts produced by blocking ions, current records were displayed, and manually controlled cursors were used to set the zero-current baseline and the open

current level, and to mark the beginning and end of a burst. A threshold was set at 50% of the unitary current amplitude and each consecutive sample point above was considered an opening and each consecutive point below was considered a closing (Colquhoun and Sigworth, 1983). Bursts were rejected when openings of more than one channel overlapped.

Some of the rapid transitions were too fast to be measured accurately with our filter setting and sampling frequency. This is true for fast blocking rates at high blocker concentrations (Figs. 2, 5, and 9) or fast unblocking rates at negative potentials (Figs. 11 and 12). In each of these cases, we have tried to make qualitative trends visible by direct inspection of the current traces, even if this called for experimental conditions under which strictly quantitative analysis was no longer possible. With the rise time of our system (0.3321/corner frequency = 0.33 ms), we were able to measure the true width of events lasting longer than ~0.3 ms (Colquhoun and Sigworth, 1983). So by not including the first bin (0–0.2 ms) in the fitting procedure, we could measure mean durations of rapidly declining exponential distributions accurately as long as there was a sufficient number of events defining the curve at intervals longer than ~0.3 ms. However, the missed events in the first bin of such a distribution will tend to artificially prolong the complementary events (e.g., prolongation of open times in the case of missed channel closings). The extent to which such concatenation occurs can be estimated by a calculation of the proportion of missed to measured short events, as shown by Colquhoun and Sigworth (1983). Using their equations, we estimate that we miss ~15% of the events with a mean duration of 1 ms (thus prolonging the complementary events by 15%), and 30% of the events with a mean duration of 0.5 ms. We have chosen to display results of kinetic analysis as apparent rates, leaving open the possibility of applying different correction procedures for missed events caused by frequency response limitations (e.g., Neher, 1983; Colquhoun and Sigworth, 1983). We have interpreted the results in a conservative way and none of our conclusions depend critically on the frequency response.

RESULTS

Discrete Interruptions in Ca Channel Current Produced by Various Blockers

Fig. 1 provides an overview of the blocking actions of Cd^{2+}, Co^{2+}, Mg^{2+}, Mn^{2+}, and La^{3+}, multivalent ions well known for their ability to inhibit Ca channels. Single Ca channel currents are evoked by depolarizing pulses from −70 to 0 mV (top trace) with 50 mM $[Ba]_o$ as the charge carrier in the patch pipette and 5 μM Bay K 8644 in the bathing solution. We used Ba^{2+} as the charge carrier because unitary current amplitudes were about twice as large as with Ca^{2+} (e.g., Hess et al., 1986). In the absence of any added blocking ion (uppermost current trace), the dihydropyridine Ca agonist promotes a form of channel gating dominated by long-lasting openings (see Hess et al., 1984, 1986, for references). With 50 mM $[Ba]_o$ as the charge carrier, the mean open time measured from sweeps with long openings was 9.1 ± 2.1 ms. When blocking ions are included along with Ba^{2+} in the pipette solution, the openings take the form of bursts of brief openings. At the concentrations illustrated, Cd^{2+}, Co^{2+}, and Mg^{2+} produce a qualitatively similar pattern of activity. Most openings and closings last enough to be fully resolved even with 1 kHz filtering, so it is clear that the unitary current amplitude is unaffected. The main difference between these ions is quantitative: Cd^{2+} is 100-fold more potent than Mg^{2+} in producing a comparable degree of block, while Co^{2+} is roughly intermediate in potency.

Blocking effects of Mn^{2+} and La^{3+} are also illustrated in Fig. 1. Mn^{2+} produces more rapid flicker than the other divalent ions; blocking and unblocking transitions are not fully resolved under the present recording conditions. As we shall discuss later, the rapidity of the transitions is consistent with the ability of Mn^{2+} to support significant currents through Ca channels (e.g., Ochi, 1975; Fukuda and Kawa, 1977; Anderson, 1983; Nelson, 1986).

As the lowest trace in Fig. 1 illustrates, the trivalent ion La^{3+} is more potent than any of the divalents in inhibiting single Ca channel activity. This is consistent with earlier studies of Ca currents in single cell or multicellular preparations

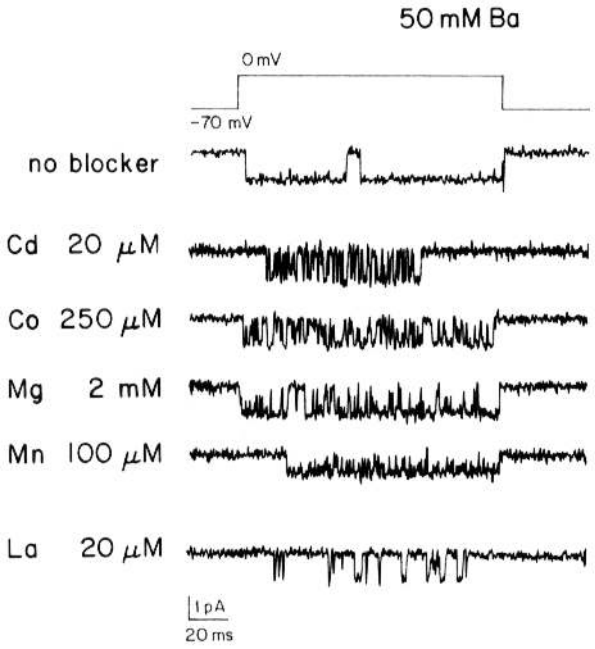

FIGURE 1. Block of single cardiac Ca channels by various inorganic ions. Current records obtained with cell-attached patch recordings from six different cells. Ca channel openings were evoked by a depolarizing test pulse (upper trace), applied every 3 s. Cells were bathed in isotonic K-aspartate to zero the membrane potential and 5 μM Bay K 8644 to induce long-lasting Ca channel openings. Patch pipettes contained 50 mM Ba^{2+} as the charge carrier, and also included blocking ions (added as chloride salts) at the concentrations indicated.

(e.g., Hagiwara, 1975; Kass and Tsien, 1975). Ca channel openings are about equally brief with either 20 μM La^{3+} or 20 μM Cd^{2+}; La^{3+} is especially effective because it produces relatively long-lasting blocking events. A further analysis of the kinetic aspects of the blocking effects of La^{3+} and a comparison with divalent ions is given later in the article (Figs. 12 and 13).

Kinetic Analysis of Cd^{2+} Block of Ba Currents

We began quantitative analysis of the mechanism of Ca channel block with Cd as an exemplary ion. Cd^{2+} is particularly interesting because it has been widely

used in the analysis of Ca channel currents and because its ionic radius (0.97 Å) is almost equal to the ionic radius of Ca^{2+} (0.99 Å).

Fig. 2 shows how the blocking effect varies with Cd concentration. The first pair of traces are control recordings with 50 mM $[Ba]_o$ and no Cd^{2+} in the pipette solution. The other current records show that discrete fluctuations between nonconducting and conducting current levels become more and more frequent

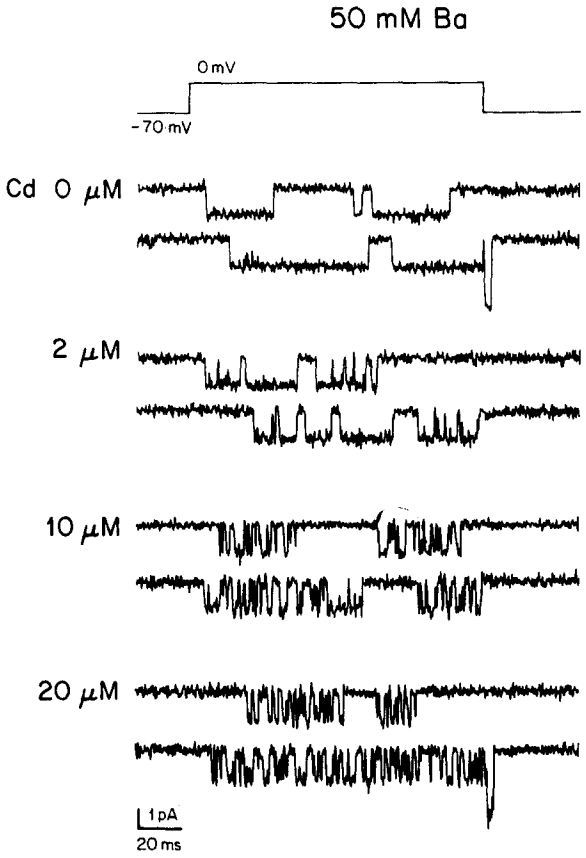

FIGURE 2. Block of unitary Ba current by varying Cd concentrations. Pairs of leak-subtracted current records from four separate cells. The patch pipettes contained 0, 2, 10, and 20 μM Cd^{2+} as indicated. Note how the number of fast closings increases as $[Cd]_o$ is raised. In the second and eighth current traces, channel openings outlast the depolarizing pulse; the unitary current increases along with the increase in driving force for Ba entry.

as $[Cd]_o$ is increased to 20 μM. With 2 μM Cd in the patch pipette, one can already begin to detect interruptions of the unitary current in excess of those brief closings found in the absence of exogenous blocker and attributed to gating transitions. With 10 or 20 μM Cd in the pipette, blocking increases to the point where the number of Cd-induced closed periods far outnumbers the closings of the channel seen in the absence of added Cd^{2+}.

For the purposes of quantitative analysis, we defined a burst as a cluster of openings separated by a closed period several times longer than the much briefer shut periods between individual openings within a burst. Once a burst was identified, the computer measured individual open and shut times within the burst as well as the length of the burst. Collected data from many bursts were used to construct histograms of the open and shut periods. Fig. 3 shows how the

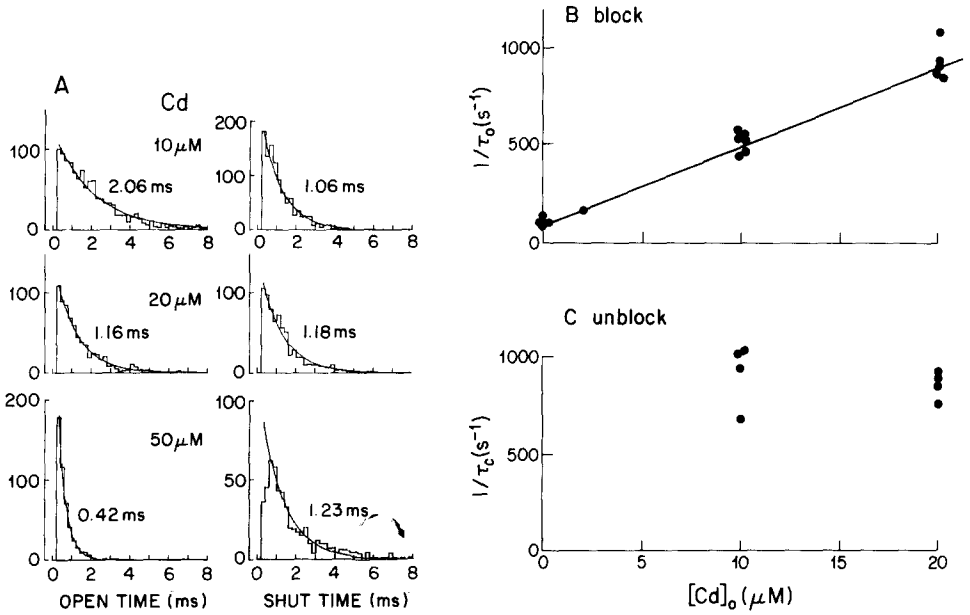

FIGURE 3. Dependence of blocking kinetics on $[Cd]_o$. Analysis of results in Fig. 2 and similar experiments. (*A*) Histograms of open and shut (blocked) times measured from bursts in three experiments in which the patch pipette contained a different Cd concentration. The ordinate plots the number of openings (left-hand panels) or the number of closings (right-hand panels). Smooth curves are single exponentials with time constants as indicated. (*B*) Shutting rate (reciprocal of the open time constant), plotted as a function of $[Cd]_o$. Each point is from a different patch. The straight line, a least-squares fit to the data with $[Cd]_o \neq 0$, intercepts the *y*-axis at 88.8 s^{-1} and has a slope of 4.04×10^7 $M^{-1}s^{-1}$. The intercept from this set of experiments is in good agreement with the points on the ordinate, which are determinations of the slow open time constant in five experiments with 50 mM Ba in the absence of Cd^{2+}. (*C*) Opening rate (reciprocal of the shut time constant) plotted as a function of $[Cd]_o$. Data at 2 μM $[Cd]_o$ were excluded from the plot because blocking events were greatly outnumbered by transitions attributed to gating.

characteristics of the distributions of open and shut times vary with Cd, using data from a different patch for each Cd concentration. We were able to compare results from different experiments because the uncertainties associated with cell-to-cell variations in resting potential were eliminated by using isotonic K-aspartate as the bathing solution (Hess et al., 1986); variations between different patches under identical ionic conditions were small.

As Fig. 3*A* illustrates, open and closed time distributions were fitted reasonably well with single exponentials (smooth curves). The values of the exponential time constants are indicated in each panel. The time constant of the open time distribution (t_o) decreased with increasing Cd concentration (left-hand histograms), whereas the time constant of the closed time distribution (t_c) remained essentially unchanged (right-hand histograms). These results are representative of collected data from 16 patches. The reciprocals of measured time constants are shown for the individual experiments in Fig. 3, *B* and *C*. t_o^{-1} increased linearly with $[Cd]_o$, while t_c^{-1} was independent of $[Cd]_o$ over the concentration range where block was readily separated from gating.

These results can be given quantitative interpretation with the help of a simple model. Within a particular burst, the kinetic behavior of the channel can be described in terms of a closed state (C2), an open state (O), and a blocked state (OB), connected in sequence as follows:

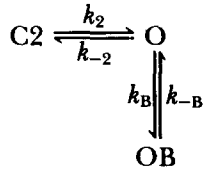

This sequential arrangement of three states has already been very useful in previous analyses of blockade of K channels (e.g., Armstrong, 1966, 1969) and acetylcholine receptor channels (e.g., Neher and Steinbach, 1978). In this particular version, k_2 and k_{-2} are the inherent, voltage-dependent rate constants for channel opening and closing, k_B is a second-order rate constant for association of the blocker (in $M^{-1}s^{-1}$), and k_{-B} is the first-order rate constant for the dissociation of the blocker. The blocking and unblocking rate constants may also be functions of voltage and permeant ion concentration (see below). C2 is the closed state immediately preceding the open state. The scheme deliberately omits C1, an additional closed state of the channel inferred from previous studies of Ca channel kinetics either in the absence or presence of Bay K 8644 (see Hess et al., 1984). C1 can be effectively ignored here because a sojourn in C1 almost always lasts long enough to terminate bursts as we define them, and therefore falls outside the analysis of intraburst kinetics.

According to the model, the distribution of open channel lifetimes in the presence of blocking ion should be a single exponential whose rate of decay should be given by the sum of the rate constants leading away from the open state:

$$t_o^{-1} = k_B[X^{++}] + k_{-2},$$

where $[X^{++}]$ is the concentration of blocking ion. This prediction of the scheme is consistent with the finding that the rate of shutting t_o^{-1} increases linearly with Cd concentration (Fig. 3*B*). The slope of the fitted line corresponds to an apparent blocking rate coefficient k_B of 4×10^7 $M^{-1}s^{-1}$. The *y*-intercept of the fitted line gives an indication of k_{-2}, the closing rate with no Cd^{2+} present.

The model attributes shut periods to sojourns in either closed or blocked states; in principle, therefore, the distribution of shut times should be a sum of

two exponentials. Resolution of both exponentials would require that the exponentials both have significant amplitudes but widely separated rates of decay. At higher Cd concentrations, where blocking transitions far outnumber closing transitions, one would expect predominance of a single exponential with rate constant k_{-B}. The results fit with this expectation: t_c^{-1} is essentially constant between 10 and 50 μM $[Cd]_o$ (Figs. 2 and 3), and presumably gives a measure of k_{-B}. We were not able to resolve two distinct exponentials at lower Cd concentrations. This is not surprising since previous estimates of k_2 are of the order of 2,000 s^{-1} (Hess et al., 1984), close to the estimate for k_{-B}.

For simplicity, the kinetic scheme ignores the possibility of C2B, a closed and blocked state, on the assumption that transitions from OB to C2B are much slower than the unblocking rate, k_B. A slow reaction connecting OB and C2B may well exist since we found no clear increase in burst length with increasing blocker concentration (cf. Neher and Steinbach, 1978).

Effect of $[Ba]_o$ on Cd Block

The results up to this point demonstrate the existence of discrete blocking events, but they are equally compatible with blocker occupancy of a regulatory site outside the pore or a blocking site along the path of permeation. To help distinguish between these possibilities, we looked for evidence of an interaction between the blocking ion and the charge-carrying ion. If, for example, Cd^{2+} and Ba^{2+} bind to the same site within the channel, competition would be expected, with less block the higher the concentration of permeant ion.

Fig. 4 shows the effects of varying $[Ba]_o$ on the block produced by a fixed concentration of Cd (20 μM). Both blocking and unblocking rates were affected: raising $[Ba]_o$ not only decreased the blocking rate (t_o^{-1}) but also increased the unblocking rate (t_c^{-1}). The change in the unblocking rate is inconsistent with a simple competition between Ba and Cd at a single external regulatory site.

We interpret these results in terms of a multiple-site, single-file pore model (e.g., Hess and Tsien, 1984, or Almers and McCleskey, 1984). For simplicity, we will assume that the pore contains only two binding sites for divalent cations, outer and inner, and that ions like Cd^{2+} and Ba^{2+} compete for the same sites. The $[Ba]_o$ dependence of the unblock rate is as expected if unblock occurs at a significant rate only when the pore contains Ba^{2+} in addition to Cd^{2+}; in this case, the rate should increase with $[Ba]_o$, since this favors double occupancy by Ba^{2+} plus Cd^{2+}. The likelihood of double occupancy of the pore can be described empirically as:

$$\text{Prob(2 ions)} = (1 + K_{app}/[Ba]_o)^{-1},$$

where K_{app} is an experimental measure of the Ba concentration that produces 50% double occupancy. Such a relationship is consistent with theoretical models of multi-site, single-file pores (e.g., Hess and Tsien, 1984, Fig. 4*d*), and has already been used to fit the $[Ba]_o$ dependence of the unitary Ba flux, which we believe to be another expression of double occupancy (Hess et al., 1986).

The $[Ba]_o$ dependence of the block rate can be explained by supposing that Cd^{2+} can only enter the pore when the outer site is vacant. Like outer-site vacancy, the rate should fall with increasing $[Ba]_o$, as observed. The likelihood

of the outer site of the pore being empty can also be roughly described by a hyperbolic function over a limited range of $[Ba]_o$. When $[Ba]_o$ is above the micromolar range, there is almost no chance that both sites in the pore will be empty. Thus,

$$\text{Prob(1 ion)} = 1 - \text{Prob(2 ions)} = (1 + [Ba]_o/K_{app})^{-1}.$$

At 0 mV, Ba ions are postulated to have equal free energy at the two sites and to equilibrate rapidly between them. Thus, the likelihood of the outer (or inner) site being empty is half of this expression:

$$\text{Prob(outer site empty)} = 0.5\ (1 + [Ba]_o/K_{app})^{-1}.$$

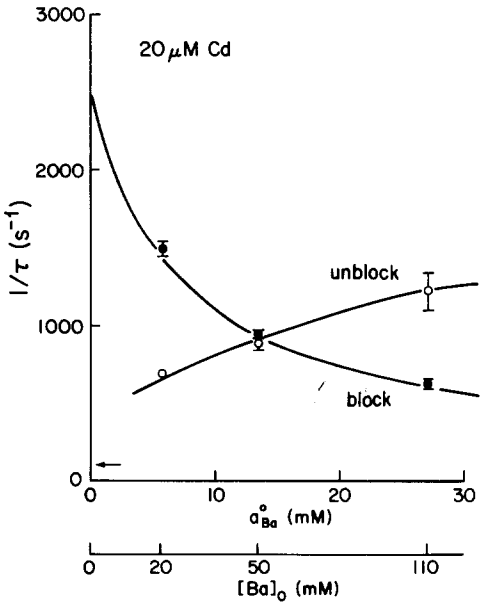

FIGURE 4. Cd blocking kinetics vary with the concentration of permeant ion ($[Ba]_o$). $[Cd]_o$ = 20 μM in all experiments. The horizontal scale is linear in Ba activity, a_{Ba}, as given in the upper scale. ●, blocking rate (t_o^{-1}). The smooth curve is a rectangular hyperbola of the form $(t_o^{-1}) = k_{-2} + k_{B,0Ba}/[1 + ([Ba]_o/K_{app})]$, where k_{-2} is set at 105 ms^{-1} (arrow), and K_{app} = 7.5 mM activity (26.2 mM $[Ba]_o$). Data points for unblocking rate (t_c^{-1}) are plotted as open symbols; the smooth curve was drawn by eye.

As Fig. 4 illustrates, this hyperbolic function provides a good fit to the blocking data, with the concentration parameter K_{app} set at 26.2 mM, a value in reasonably close agreement with 27.9 mM, the K_{app} for the Ba dependence of unitary Ba current (Hess et al., 1986, Fig. 7).

The theoretical fit to the blocking data provides a basis for estimating the entry rate for Cd^{2+} in the absence of interaction with permeant ions. Extrapolating to low millimolar Ba concentrations where Prob(outer site empty) = 0.5, the y-intercept in Fig. 4 is 2,500 s^{-1}; since $[Cd]_o$ = 20 μM, the calculated primary Cd entry rate coefficient is

$$(2{,}500\ s^{-1})/(20\ \mu M)(0.5) = 2.5 \times 10^8\ M^{-1}s^{-1}.$$

This value is to be compared with the entry rate for Ca^{2+} given below (p. 336).

Block of Ba Currents by Mg^{2+}

Mg ion is the main inhibitor of Ca current under physiological conditions, and variations in $[Mg]_o$ have been used for many years in the analysis of Ca^{2+}-dependent processes such as transmitter release (e.g., Douglas, 1968; Katz, 1969).

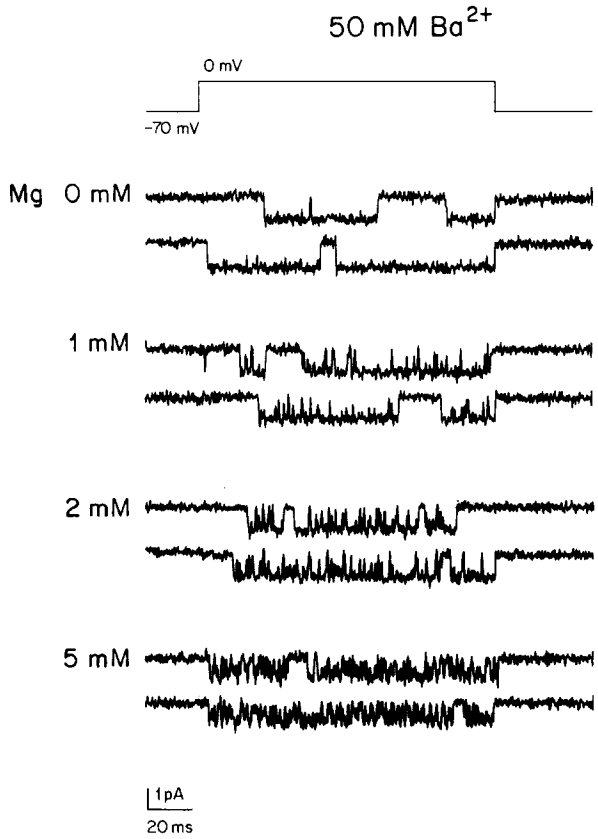

FIGURE 5. Block of Ba currents by Mg^{2+}. Representative current traces from four cells where the patch pipette contained 50 mM Ba^{2+} and 0, 1, 2, or 5 mM Mg^{2+} as indicated.

Mg inhibition of Ca currents has been attributed to reduction of the local Ca concentration through screening of negative surface charge (Muller and Finkelstein, 1974); others have argued that Mg^{2+} interacts with specific blocking sites but that it has the lowest affinity among divalent cations that act as blockers (e.g., Hagiwara and Takahashi, 1967; Akaike et al., 1979; Fukushima and Hagiwara, 1985).

Fig. 5 shows that Mg block of Ba currents can be resolved at the single channel level as discrete events. Unlike Cd^{2+}, which blocks at micromolar concentrations

with 50 mM $[Ba]_o$ as the charge carrier (Fig. 2), Mg^{2+} produces appreciable block only at concentrations of ~1 mM or greater; the half-blocking concentration under these conditions is ~10 mM. The relative weakness of Mg^{2+} as a blocker is due in part to the brevity of the closed periods. As illustrated in the bottom traces in Fig. 5, the rate of block also becomes very fast at concentrations of ≥5 mM, and individual openings and closing become hard to resolve.

Histograms of open and shut times were determined for a range of Mg concentrations (not shown). As in the case of Cd^{2+}, distributions were fitted well by single exponentials; the time constants for the distributions of open times

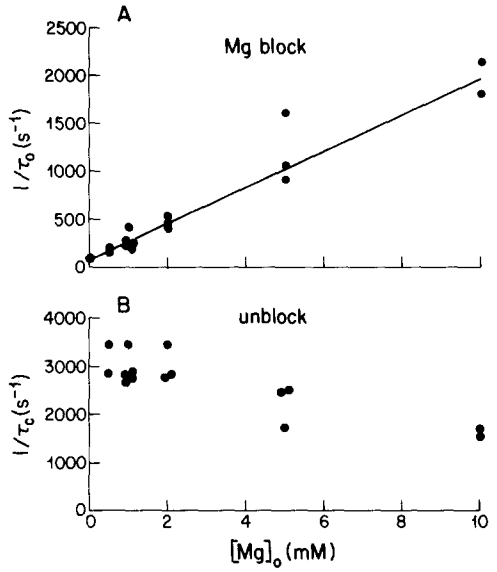

FIGURE 6. Dependence of blocking kinetics on $[Mg]_o$. Open and shut time histograms from experiments like those shown in Fig. 5 were fitted with single exponentials. (*A*) Shutting rate (measured as the reciprocal of the open time constant) plotted as a function of $[Mg]_o$. Each data point is from a different patch. The straight line, a least-squares fit of the data with $[Mg]_o \neq 0$, has a slope of 1.90×10^5 $M^{-1}s^{-1}$ and a *y*-intercept of 78.2 s^{-1} ($r = 0.99$). The data point for $[Mg]_o = 0$ is the mean of five experiments with pipettes containing 50 mM Ba^{2+} and no added blocker (see Fig. 3*B*). (*B*) Opening rate (reciprocal of the shut time constant) plotted against $[Mg]_o$.

became briefer as the Mg concentration in the pipette was raised, while the distributions of shut times were not strikingly changed. Fig. 6 displays collected results from 20 patches and shows that the overall $[Mg]_o$ dependence is similar to the $[Cd]_o$ dependence in Fig. 3. The blocking rate t_o^{-1} increases as a linear function of $[Mg]_o$ with a slope that corresponds to an apparent blocking rate coefficient of 1.9×10^5 s^{-1}, ~200-fold slower than Cd^{2+}. The unblocking rate t_c^{-1} shows little dependence on $[Mg]_o$ below 2 mM, although at higher concentrations the rate of unblocking becomes somewhat slower.

As in the case of Cd block, Mg block is strongly dependent on the concentration of the charge carrier. Increasing $[Ba]_o$ strongly decreases the rate of block and

increases the rate of unblock (Fig. 7). This suggests again that both blocking and unblocking steps are sensitive to the presence of permeant ions, presumably within the pore itself. The data on Mg block are the hardest to analyze quantitatively, because the rapid off rates give rise to partially resolved blocking transitions. We have therefore restricted our analysis of Mg block to the observation of qualitative trends and have not attempted to extract a value for the absolute entry rate coefficient by extrapolation to zero $[Ba]_o$.

Block of Ba Currents by Ca^{2+}

The next series of experiments focused on the blocking actions of the Ca ion itself. It is well known that Ca^{2+} can inhibit Ca channel current carried by other divalent ions such as Sr^{2+} (Vereecke and Carmeliet, 1971) or Ba^{2+} (Hess et al., 1983; Almers and McCleskey, 1984). In general, Ca^{2+} seems to have a higher

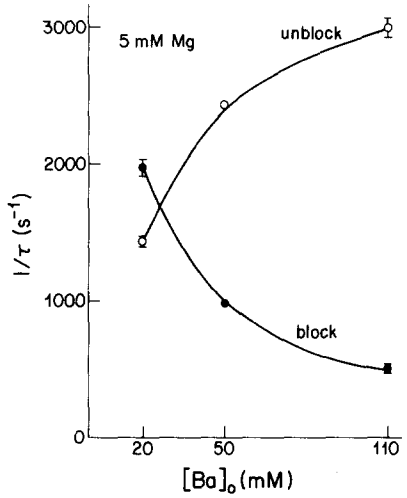

FIGURE 7. Mg blocking kinetics vary with $[Ba]_o$. $[Mg]_o$ = 5 mM, $[Ba]_o$ as indicated. Values of t_o^{-1} are from individual patches plotted as solid circles; t_c^{-1} values are plotted as open circles. Smooth curves were drawn by eye.

affinity for Ca channels than these other ions (Hagiwara et al., 1974). Fig. 8*A* shows block of Ba currents by Ca^{2+} at the level of unitary currents. Records were obtained from three patches with pipettes containing a constant background of 50 mM Ba. The addition of 5 or 10 mM Ca produced a graded reduction in the amplitude of the unitary current without detectable flickering. Fig. 8*B* plots collected results from 28 patches over a wider range of Ca concentrations; the decrease in unitary current size is a graded function of $[Ca]_o$; with $[Ba]_o$ = 50 mM, ~10 mM $[Ca]_o$ is needed to reduce the unitary current amplitude to 50% (solid symbols). For comparison, the open symbols show the amplitude of the unitary current with only Ca^{2+} present.

The fact that no individual blocking events could be resolved over the range of Ca concentrations tested (10 μM to 50 mM) is most easily explained by an unblocking rate that greatly exceeds the dynamic range of our measurements.

With a high unblocking rate, effective block requires an equally high blocking rate (achieved at high blocker concentrations). The resulting very rapid blocking and unblocking transitions are then seen as an overall reduction in unitary current, corresponding to an equilibrium between open and blocked states. Our observation of a very rapid unblocking rate for Ca^{2+} in the presence of high

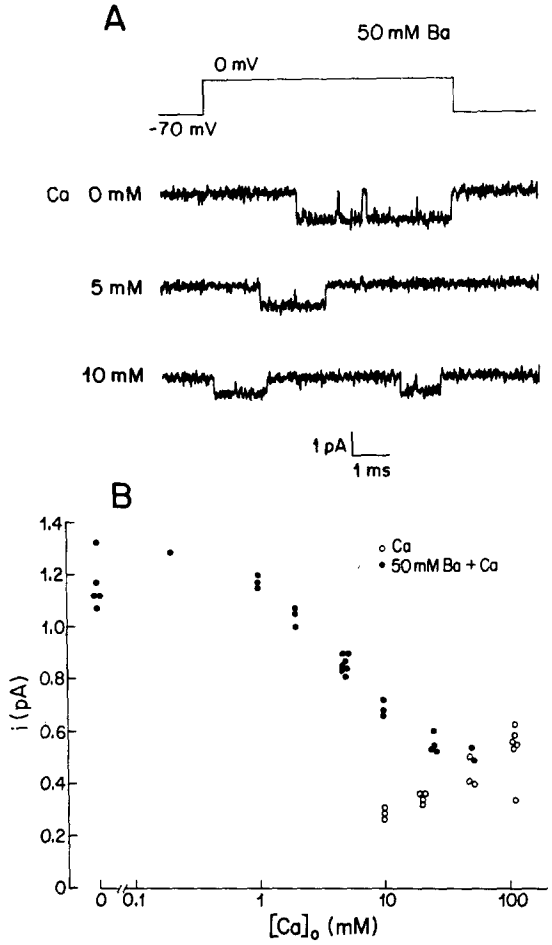

FIGURE 8. Block of unitary Ba current by Ca^{2+}. (*A*) Current records from three patches in which the pipette contained 50 mM Ba^{2+} plus 0, 5, or 10 mM Ca^{2+}. (*B*) Measurements of unitary current amplitude. Pipettes contained 50 mM Ba^{2+} plus the Ca concentration indicated on the abscissa (solid circles) or various Ca concentrations in the absence of Ba^{2+} (open circles).

$[Ba]_o$ fits nicely with recent hypotheses that postulate ion-ion interactions within the Ca channel pore (Hess and Tsien, 1984; Almers and McCleskey, 1984). These hypotheses suggest that Ca is permeant by virtue of its ability to leave the pore rapidly when the pore is multiply occupied by divalent cations; such multiple occupancy should be pronounced when the external solution contains 50 mM Ba.

Block of Monovalent Currents by Ca^{2+}

This line of reasoning suggests that discrete block by Ca ions might be detected at low divalent cation concentrations if a monovalent cation serves as the Ca channel charge carrier. It is well known that monovalent cations can support large currents through Ca channels when the extracellular Ca concentration is reduced to submicromolar levels (Kostyuk and Krishtal, 1977; Kostyuk et al., 1983; Hess and Tsien, 1984; Almers et al., 1984); in the preceding article (Hess

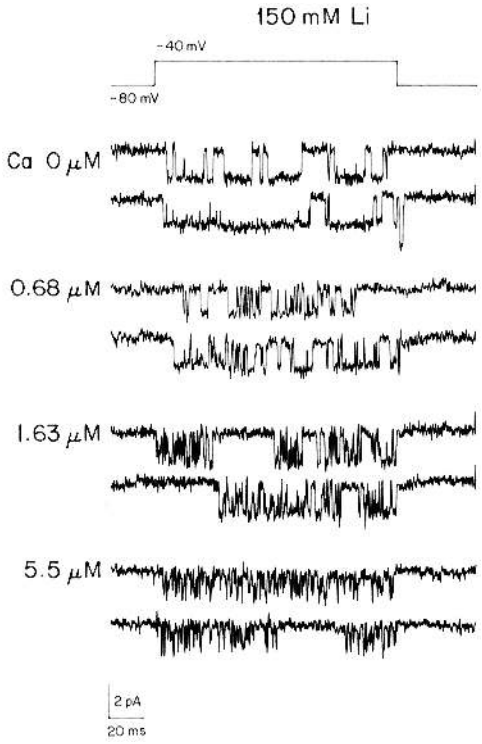

FIGURE 9. Block by Ca^{2+} of unitary Li current through the Ca channel. The patch membrane potential was stepped from −80 to −40 mV (upper trace). Unitary currents carried by Li influx through the Ca channel (top, left) were measured with 150 mM LiCl, 10 mM EGTA, and 12.5 μM TTX in the patch pipette. The Ca concentration of the patch pipettes was buffered to the values indicated with H-EDTA ($K_{D,Ca}$ = 1.63 μM at pH 7.5).

et al., 1986), we show that Na or Li currents through the Ca channel can be resolved at the single channel level.

Fig. 9 illustrates Ca block of unitary Li currents. We used Li^+ rather than Na^+ as the charge carrier to avoid possible interference from proton block of Na current through Ca channels (see Hess et al., 1986). The top panel shows Li currents recorded with a pipette solution containing no added divalent ions and 2 mM EGTA ($[Ca]_o < 0.01$ μM). Three lines of evidence suggest that the unitary currents are due to Ca channels and not Na channels (see also Hess et al., 1986):

(*a*) the pipette solution contained 12 μM TTX, (*b*) mean currents formed as averages of many sweeps showed a time course appropriate for Ca channels and not Na channels, and (*c*) the voltage dependence of activation and inactivation was as expected for Ca channels.

Blocking events could just be detected at 0.68 μM $[Ca]_o$, and became more pronounced at 1.63 μM $[Ca]_o$. At 5.5 μM $[Ca]_o$, current records appeared as a

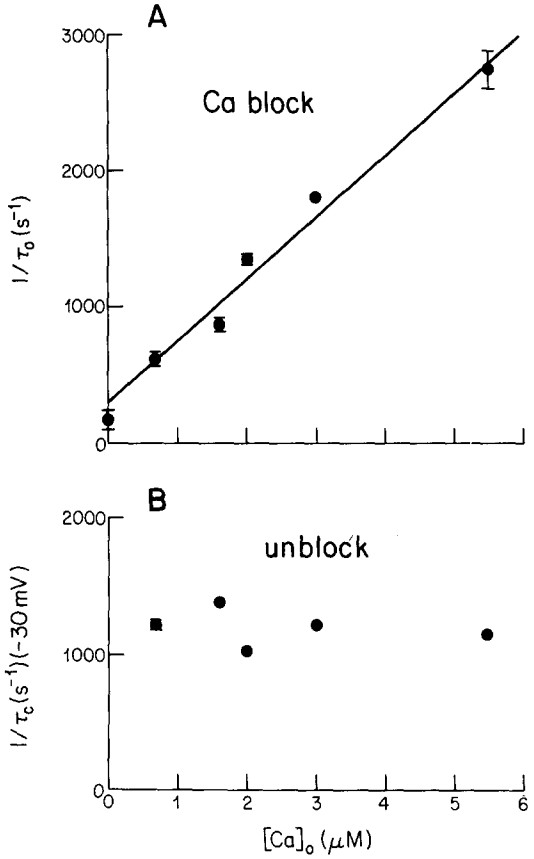

FIGURE 10. Concentration dependence of Ca block of Li current through the Ca channel. (*A*) Reciprocal of the open time constant plotted as a function of $[Ca]_o$. The line is a least-squares fit through the data points (slope, 4.51×10^8 $M^{-1}s^{-1}$; *y*-intercept, 305 s^{-1}). Exclusion of the point at 5.5 Ca_o yields a regression value for the slope of 5.1×10^8. (*B*) Reciprocal of the closed time constant plotted as a function of $[Ca]_o$.

rapid series of spike-like events. Histograms of open and closed times (not shown) were fitted by single exponentials as expected for a single open and a single blocked state. Fig. 10 plots collected results from a large number of patches. The blocking rate (t_o^{-1}) increases linearly with $[Ca]_o$ (*A*), while the rate of unblock is independent of $[Ca]_o$ (*B*). The *y*-intercept of the regression line corresponds to an open time of 3.3 ms, a value that is not significantly different from the mean

open time of 5.8 ms measured in the absence of Ca^{2+} and indicated by the symbol on the ordinate. The slope of the regression line corresponds to an apparent rate of 4.5×10^8 $M^{-1}s^{-1}$. This value gives an estimate of the primary rate coefficient of Ca entry, which would apply if Li^+ were to bind so weakly to the channel that Ca^{2+} enters and leaves an essentially empty pore. If, as seems more likely, Li^+ binds significantly to the pore, this value would be a lower limit.

Voltage Dependence of Block by Ca_o

The voltage dependence of the rates of blocking and unblocking gives information on the relative locations of the energy barriers and wells an ion encounters as it moves through a channel. From the effects of voltage on the individual entry and exit rates, we can see which steps in the permeation process are responsible for the voltage dependence of steady state block.

Fig. 11 shows recordings of Li current through Ca channels taken at −30 (*A*) and −60 mV (*B*) in the absence and presence of Ca_o. It is evident that hyperpolarization abbreviates Ca-induced blocking events, to the extent that many of the shut periods are incompletely resolved. Analysis of such records gives the histograms shown in Fig. 11*C*. The shut time distribution at −60 mV decays much more quickly than the distribution of shut times at −30 mV. This trend is borne out by collected analysis of results from seven patches. Fig. 11*D* shows the voltage dependence of the individual blocking and unblocking rate constants. The blocking rate (t_o^{-1}) shows very little dependence on voltage over the potential range we examined. On the other hand, the rate of unblocking (t_c^{-1}) shows strong voltage dependence, increasing e-fold with ~40 mV hyperpolarization. An increase in the rate of exit of Ca with hyperpolarization would be expected since Ca^{2+} is a permeant ion and can exit into the cell interior. The almost negligible voltage dependence of the entry rate indicates that the transition state for the entry of Ca^{2+} into the channel occurs outside of the electric field.

Voltage-dependent Block of Unitary Ba Current by Cd_o, La_o, and Mg_o

Previous work has shown voltage dependence of the degree of steady state block by external Cd^{2+} (Byerly et al., 1985) or Mg^{2+} (Fukushima and Hagiwara, 1985). Byerly et al. noticed that hyperpolarization decreased the degree of Cd block in snail neurons, and suggested that Cd^{2+} might escape into the cell. Fukushima and Hagiwara (1985) found that Mg inhibition increased with hyperpolarization, and suggested that Mg^{2+} might be trapped deeper in the pore. Single channel recordings have afforded us the possibility of determining the voltage dependence of individual blocking and unblocking rates.

Fig. 12 shows representative current records illustrating the influence of membrane potential on the blocking effects of Cd^{2+}, La^{3+}, and Mg^{2+} on unitary Ba currents. To varying degrees, the voltage dependence is similar to that seen with Ca block of unitary Li currents. Voltage dependence was demonstrated in most experiments by varying the test potential level (as in Fig. 12, *E* and *F*). We also took advantage of Bay K 8644–promoted channel openings that outlast the depolarizing pulse. In the absence of added blocking ion (Fig. 12*A*), such openings are expressed as large tail currents (~3.5 pA) at the holding potential. Block of tail currents displayed different characteristics than block of the current

during the test pulse itself. For example, panel *B* shows unitary Ba currents with 20 μM Cd^{2+} in the recording pipette. Whereas unitary currents recorded during the test pulse to 0 mV show substantial block, the tail current recorded at −70 mV was much less affected; the duration of the blocking events was clearly briefer, and the degree of block was less severe.

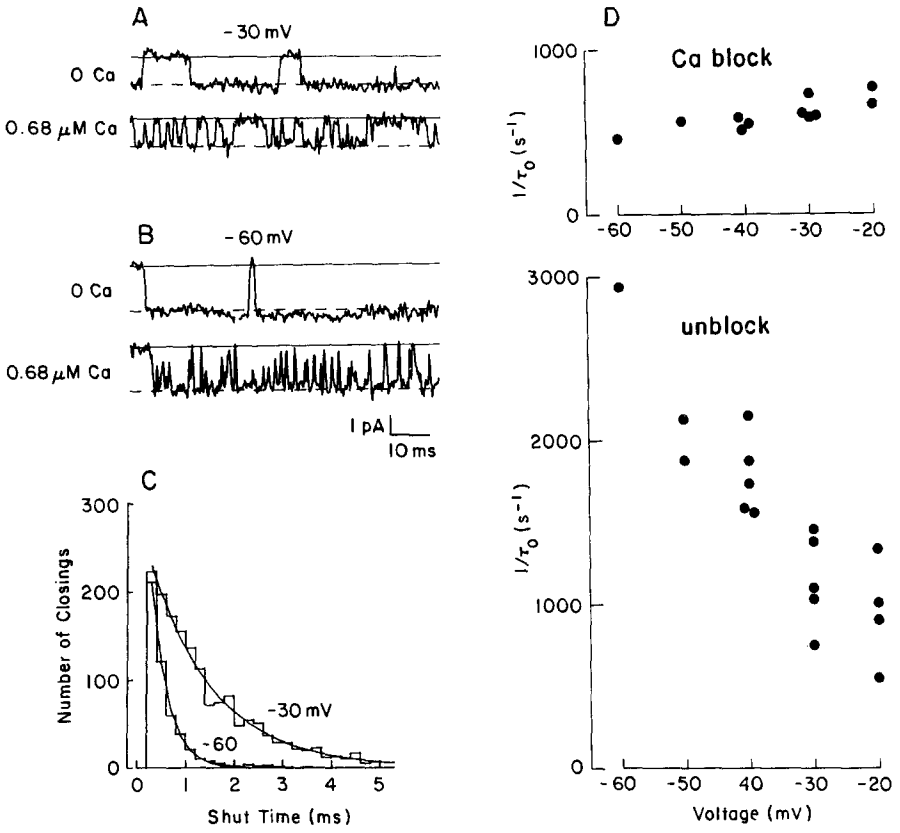

FIGURE 11. Voltage dependence of Ca block of unitary Li currents. (*A*) Current records at −30 mV from two patches where the pipette contained 150 mM Li^+ and either 0 (top) or 0.68 μM Ca^{2+} (bottom). (*B*) Same two patches at −60 mV. (*C*) Histograms of shut times within bursts with 0.68 μM Ca^{2+} in the pipette (same experiment as in *A* and *B*). Smooth curves are single exponentials with time constants of 1.33 ms at −30 mV and 0.34 ms at −60 mV. (*D*) Voltage dependence of shutting rate (inverse of the open time constant) with 0.68 μM $[Ca]_o$ (top) and voltage dependence of opening rate (reciprocal of shut time constant) with 0.68–1.36 μM $[Ca]_o$ (bottom).

Panels *E–H* illustrate the voltage dependence of block by La^{3+}. At 0 mV (*E*), the blocking events are so long-lasting that they are difficult to distinguish from channel closings. The presence of a tail following the end of the clamp pulse provides a strong clue that the channel exhibited mode 2 gating during the pulse and that the relatively long shut periods are due to La block. At −20 mV (the

test potential in *F*), bursts of openings can usually be identified without much difficulty. At −50 mV (the potential following the test pulse in panel *G*), the tail current appears as a well-defined burst of openings and La-induced blocking events. At −90 mV (the "tail" potential in *H*), the rate of unblock becomes so rapid that most blocked periods are not fully resolved.

Fig. 13 shows collected results from experiments on block by Cd^{2+} (*A*) and

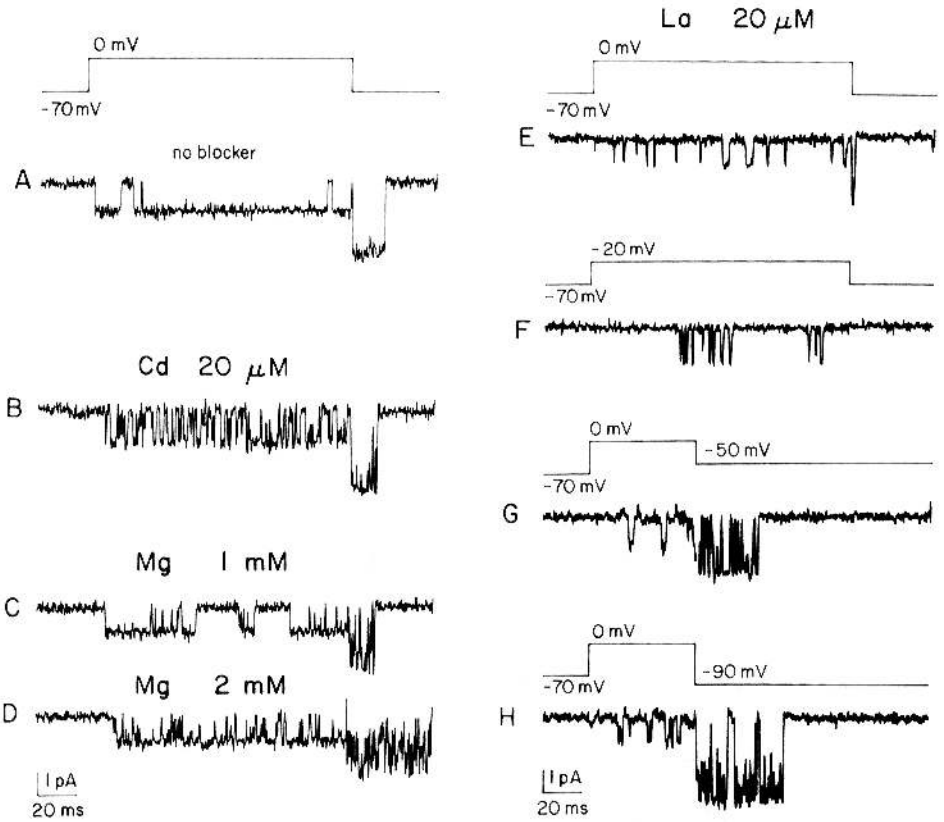

FIGURE 12. Block of Ba current by Cd^{2+}, Mg^{2+}, and La^{3+} at different membrane potentials. Comparison of blocking characteristics at different test pulse potentials or at different potentials for "tail" current following test pulses. Left-hand traces show current records from four patches, with no blocker (*A*), or with patch pipettes containing 20 μM Cd^{2+} (*B*), 1 mM Mg^{2+} (*C*), or 2 mM Mg^{2+} (*D*). Traces *E–H* were recorded from a patch with 20 μM La^{3+} in the pipette solution.

La^{3+} (*B*). In both cases, the blocking rate t_o^{-1} remains near 10^3 s^{-1} over a range of 40–60 mV. On the other hand, the unblocking rate t_c^{-1} increases strongly with hyperpolarization. In this respect, Cd or La block of Ba currents resembles Ca block of Li currents. Interestingly, the voltage dependence with Cd^{2+} and La^{3+} is similar (e-fold per 20–25 mV), despite the difference in valence between these ions.

The voltage dependence of block is different for Mg^{2+} than for the other ions we studied. The voltage dependence is illustrated by traces taken with 1 mM $[Mg]_o$ (Fig. 12 *C*) and 2 mM $[Mg]_o$ (Fig. 12 *D*). Membrane hyperpolarization does not lessen the degree of steady state block, as in the case of Cd^{2+} or La^{3+}; steady state block is actually more severe at negative potentials, as reported by Fukushima and Hagiwara (1985). The kinetic basis for this effect of hyperpolarization can be seen by comparing the pattern of opening and closing at the pulse

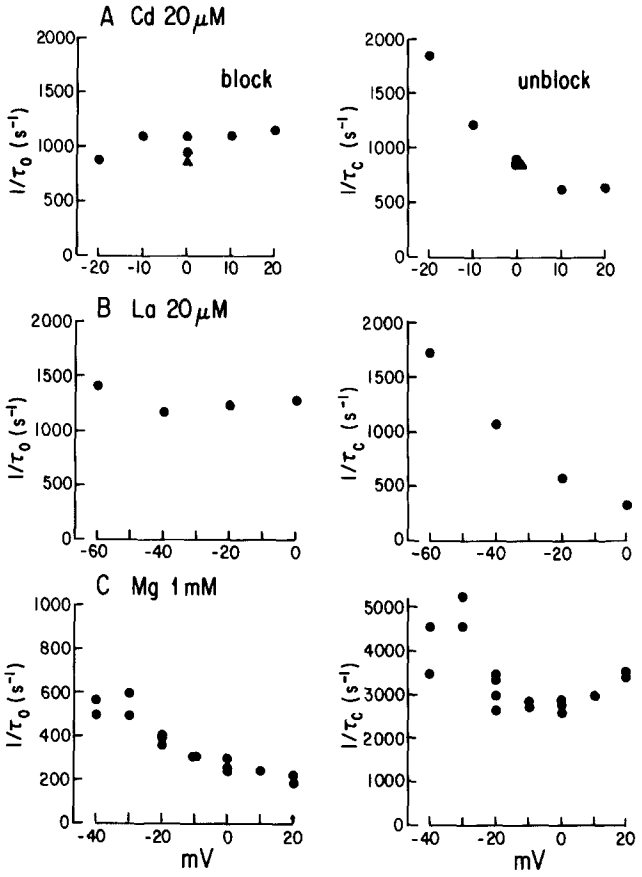

FIGURE 13. Voltage dependence of block of Ba currents by Cd^{2+}, La^{3+}, and Mg^{2+}. Reciprocals of open time distribution time constants (left panels) and closed time distribution time constants (right panels) for block of Ba current by 20 μM $[Cd]_o$ (*A*), 20 μM $[La]_o$ (*B*), and 1 mM $[Mg]_o$ (*C*).

potential and at the potential where tail current is recorded. The current signal flickers more at −70 than at 0 mV. This corresponds to a marked acceleration of both opening and closing transitions with hyperpolarization. Collected data from five patches (Fig. 13 *C*) show that these changes in the blocking kinetics of Mg^{2+} were a consistent finding. The plot may underestimate the true voltage

dependence of the blocking rate; at negative potentials, many of the closings are brief enough to be missed.

DISCUSSION

The main advance in this article is the resolution of individual rates of channel block and unblock. The results suggest that Ca^{2+}, Cd^{2+}, Mg^{2+}, Co^{2+}, Mn^{2+}, and La^{3+} can inhibit current flow through Ca channels by lodging within the pore itself. Analysis of rates of block and unblock thus provides new information about mechanisms of ion selectivity and permeation. The results are generally consistent with earlier studies of whole cell macroscopic currents, which described the equilibrium between blocked and unblocked channels but not individual rates (e.g., Byerly et al., 1985; Fukushima and Hagiwara, 1985).

In previous studies of unitary Ca channel current, block took the form of a reduction in unitary current amplitude rather than discrete blocking and unblocking transitions (Nelson et al., 1984; Matsuda, 1986). The contrast with our results is easily explained by differences in experimental conditions. Nelson et al. studied block by La^{3+}, Cd^{2+}, and Mn^{2+} with 250 mM Sr^{2+} as the charge carrier; channel unblock was probably even faster than with 50 mM Ba (Fig. 4), and might easily have escaped resolution with the 50 Hz filtering used for bilayer recording. Matsuda (1986) recorded unitary Na currents through Ca channels without the benefit of Ca agonist to prolong channel openings; unitary events were brief and often incompletely resolved even in the absence of block, so rapidly flickering block could have appeared as a reduction in unitary amplitude.

Tests of Hypotheses for the Mechanism of Block

Our experiments do not support the idea that Mg^{2+} inhibits Ca current by reducing the local Ca concentration through screening of negative surface charges without specific binding of ions (Muller and Finkelstein, 1974). This hypothesis predicts that increasing $[Mg]_o$ should produce a graded reduction in the amplitude of the unitary flux, rather than the discrete interruptions in single channel current that were actually observed.

The present results are also at variance with the double selectivity filter hypothesis of Kostyuk et al. (1983). They postulated a high-affinity regulatory site ($pK_{Ca} \sim 6.6$) outside the channel, where binding of divalent cations triggers conformational changes that render the pore impermeable to monovalent cations, and a low-affinity selectivity site ($pK_{Ca} \sim 2.0$) that confers selectivity among various divalent cations. A number of experimental observations cannot be accounted for by the hypothesis as originally stated. (*a*) Since the proposed regulatory site is external, and not in the permeation path, the hypothesis does not predict that hyperpolarization should increase the rate of removal of Ca block of Li current, as actually observed (Fig. 11). (*b*) With a high-affinity site that is quickly saturated at low $[Ca]_o$ or $[Ba]_o$, and only one low-affinity site, the model cannot account for the finding that raising $[Ba]_o$ speeds the removal of block by Cd^{2+} or Mg^{2+} (Figs. 4 and 7). (*c*) Observations of "anomalous mole fraction" effects (Hess and Tsien, 1984; Almers and McCleskey, 1984) are also difficult to explain with only one intrapore binding site. Several additional ad hoc assumptions would be required to bring this hypothesis into line with the experimental data.

All of the results in this article seem consistent with the idea that the Ca channel is a single-file pore, and that "blocking" ions compete with "permeant" ions for multiple binding sites within the pore (Hess and Tsien, 1984; Almers and McCleskey, 1984). This hypothesis is simpler than the scheme of Kostyuk et al. (1983). Although it also requires a minimum of two ion binding sites, blocking effects can be accounted for by the same kind of ion-pore and ion-ion interactions that are thought to occur during permeation. There is no need to postulate different properties for the sites, or special interactions between sites other than the expected coulombic repulsion between positively charged ions.

The observation that hyperpolarization increases the rate of unblock of Li current by Ca^{2+} is accounted for by a direct effect of electric field, driving blocking Ca ions out of the pore into the cytoplasm. The fact that elevating $[Ba]_o$ not only decreases the rate of Cd or Mg block, but also increases the rate of unblock, fits with the idea of at least two intrapore binding sites. The finding that the rate of Ca unblock is slow and easily resolved when the divalent cation concentration is low (Fig. 9), and too fast to be resolved when the divalent cation concentration is high (Fig. 8), is to be expected if the departure of Ca^{2+} were speeded by interaction (electrostatic or otherwise) with other divalent cations that enter the pore.

Block and Permeation as Different Expressions of Ion-Pore Interactions

From these results and earlier studies, one may conclude that there is no absolute distinction between "blocking" and "permeant" ions, but only quantitative differences among inorganic ions in the rates at which they enter and leave the pore. The fact that permeant ions can act as blockers is already well known. Ca^{2+} and other divalent ions are potent inhibitors of monovalent ion currents; Ca^{2+} is permeant but can block Sr or Ba currents (e.g., Vereecke and Carmeliet, 1971); similarly, Mn^{2+} is permeant but can inhibit Ca currents (e.g., Ochi, 1975). Our experiments provide additional information suggesting that the converse is also true: Cd^{2+}, Mg^{2+}, Co^{2+}, and La^{3+}, ions that are usually classified as blockers of cardiac Ca channel currents, may also be slightly permeant. In each case, the marked speeding up of the unblocking reaction with hyperpolarization strongly suggests that these ions are able to escape from the pore to the cytoplasm (see also Byerly et al., 1985). The response to hyperpolarization could be due to a direct electric force on the blocking ion or an indirect effect, involving increased permeant ion occupancy at an outer pore site and possible repulsive interactions with the blocking ion.

Although previous experiments have shown Mg current though Ca channels of vertebrate skeletal muscle (Almers and Palade, 1981; Affolter and Coronado, 1985) and Cd current in insect skeletal muscle (Fukuda and Kawa, 1977), patch-clamp recordings have failed to produce direct evidence for Cd or Mg current in heart cells (Hess et al., 1986) or neoplastic B lymphocytes (Fukushima and Hagiwara, 1985). The results in heart cells are to be expected: rates of Cd or Mg unblock of the order of 10^3–10^4 s^{-1} correspond to currents small enough to escape detection by direct electrical recording. Evidence for Cd, Mg, or La influx via Ca channels might be obtained with methods that measure intracellular ion accumulation. Tests for Ca channel permeation would be particularly important

in the case of La, since La ions have long been used as markers for extracellular Ca binding sites. Our results suggest that La may also reach sites within the pore and the cytoplasm.

Ca Block Gives Information about the First Step in Permeation

The rate of Ca block of Li currents can be expressed as a second-order rate coefficient of 4.5×10^8 $M^{-1}s^{-1}$. On the basis of arguments presented above, we take this blocking rate as a direct measure of Ca entry into the channel, the first stage of ion permeation. If this interpretation is correct, our data give the first estimate of the rate of primary interaction between a pore and its favored physiological ion. The measured value is, if anything, a lower limit because it ignores Li binding to channel sites.

The entry rate coefficient is about six times faster than an effective rate coefficient for the overall ion transfer process, 7.5×10^7 $M^{-1}s^{-1}$, derived from a measurement of a unitary Ca flux at 10 mM Ca of 750,000 s^{-1} (Hess et al., 1986). The simplest interpretation is that Ca entry is not rate-limiting in the overall process of ion transfer.

It is interesting to compare the measured on rate with theoretical expectations for the diffusion-limited rate of ionic collisions with the mouth of the pore, namely

$$k = 2\pi rDN \cdot 10^{-3},$$

where r is the capture radius in centimeters, D is the diffusion coefficient of Ca in free solution (8×10^6 cm^2s^{-1}), and N is Avogadro's number. A reasonable estimate for r can be obtained by taking the difference between the radius of tetramethylammonium, the largest ion known to permeate Ca channels (McCleskey and Almers, 1985; McCleskey et al., 1985) and the radius of a Ca ion. This gives $r = (2.75\ \text{Å} - 1.0\ \text{Å}) = 1.75$ Å, and a calculated on rate of $k = 5.3 \times 10^8$ $M^{-1}s^{-1}$.

The close agreement with the measured value is probably fortuitous. For one thing, the calculation ignores the influence of electrostatic forces on the interaction between Ca ions and the pore mouth (see Hille, 1984; Moore and Pearson, 1981). The main point is that the measured value of k is of the same order as theoretical expectaions for diffusion control. We found other evidence consistent with a diffusion-limited on rate. Like the on rate for Ca^{2+}, the on rates for Cd^{2+} and La^{3+} were very fast, and within a factor of 2 of the Ca on rate if allowance is made for Ba occupancy of the channel as in Fig. 4. As in the case of Ca^{2+}, Cd and La on rates were essentially voltage independent, as expected for a process that occurs outside the membrane field.

What Determines an Ion's Effectiveness as a Permeator or Blocker?

Fig. 14 classifies the ions we have examined according to their effectiveness in blocking the channel (this article) or carrying charge through it (Hess et al., 1986). Starting in the upper left-hand corner and moving clockwise, the ions range from those that are potent blockers and are not detectably permeant (e.g.,

Cd^{2+}), to ions that are potent blockers and are easily permeant (e.g., Ca^{2+}), to ions that are easily permeant but are not effective as blockers (e.g., Na^{+}).

Since Cd^{2+}, Ca^{2+}, and Na^{+} have almost identical Pauling radii, it is evident that this spectrum of behavior does not arise from considerations of ionic size alone (see also McCleskey and Almers, 1985). Instead, we propose that this progression largely reflects differences in ion affinity for the proposed intrapore binding sites: very high-affinity binding gives potent block but a dissociation so slow that fluxes are immeasurably small; very low-affinity binding leads to large fluxes and no block; binding with intermediate strength in the micromolar range makes Ca^{2+}, Sr^{2+}, and Ba^{2+} potent as blockers of monovalent ion fluxes, but allows reasonably large divalent fluxes with the help of a negatively cooperative interaction such as electrostatic repulsion between pairs of ions.

Mg^{2+} is both a weak blocker and a poor permeator, and thus lies in a distinct category outside the sequence described so far. We attribute this behavior to the slowness of the primary association between Mg^{2+} and the pore. This is in accord with experimental measurements of the rate constants for Mg or Ca complex

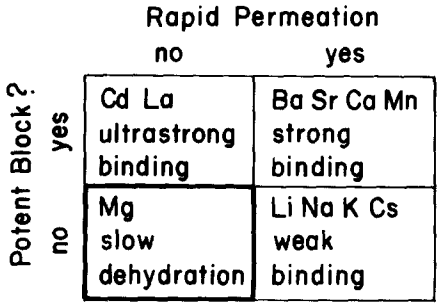

FIGURE 14. Classification of ions as blockers or permeators.

formation with ligands of known structure, which give typical values of 5×10^5 $M^{-1}s^{-1}$ for Mg^{2+} as opposed to 5×10^8 $M^{-1}s^{-1}$ for Ca^{2+} (Hague, 1977). It is believed that Mg^{2+} differs from Ca^{2+} and Cd^{2+} because of its interaction with water, the rate of exchange of water molecules on its inner shell of hydration being three or four orders of magnitude slower than for the other ions in Fig. 14 (Diebler et al., 1969). Loss of water seems to be a rate-limiting step in a series of steps: (*a*) the association of fully hydrated ion with ligand in a loose complex with a dissociation constant of the order of 1 M, (*b*) a loss of one water molecule from the ion's inner hydration sphere, (*c*) the development of a strong interaction between metal ion and ligand (Hague, 1977).

Mg^{2+} is also exceptional in the voltage dependence of its blocking rate, which increases e-fold per 55 mV hyperpolarization. This voltage dependence is as expected for an outer energy barrier located 20% down the electrical field. One possible explanation for the contrast with other ions is that Mg^{2+} penetrates further into the pore before experiencing stabilization from ligand groups exchanging with water, perhaps because of its smaller size or slower rate of dehydration.

Inferences about Channel Structure

Previous articles have compared putative Ca binding sites in the Ca channel to high-affinity binding sites on calcium-binding proteins such as calmodulin or troponin (Kostyuk et al., 1983; Hess and Tsien, 1984; Almers and McCleskey, 1984) or on Ca chelators such as EGTA (Hess and Tsien, 1984). Table I shows various similarities and differences in (*a*) the rate coefficient of Ca association with or dissociation from various binding sites, and (*b*) the relative affinity for Ca^{2+} and other polyvalent ions. Our value of k_{on} for Ca channels is somewhat faster than estimates of k_{on} for biological Ca binding proteins like troponin. It is most similar to values for quin 2, azo 1, and fura 2, members of a family of derivatives of BAPTA, a Ca chelator structurally related to EGTA (Tsien, 1980).

TABLE I

Comparison of Ca Channels and Other Ca Binding Molecules

Molecule	Rates of Ca association and dissociation		Reference
	Association	Dissociation	
	$10^8\ M^{-1}s^{-1}$	s^{-1}	
Ca pore (−30 mV)	4	1,200	This paper
Quin 2	7.5	57	Bayley et al., 1984
Azo 1	4	1,200	R. Y. Tsien and J. Kao, personal communication
Fura 2	6	100	"
Parvalbumin	1.2	0.5	Potter et al., 1978
Troponin C	~1	312	Potter and Johnson, 1982
Calmodulin	—	550	Bayley et al., 1984
	Relative affinities for Ca and other ions		
Ca pore (L)	Cd > Ca ~ Sr > Ba > Mg		This paper
EGTA	Cd > Ca > Sr ~ Ba > Mg		Martell and Smith, 1974
Quin 2	Ca > Sr > Mg		Hesketh et al., 1983
Parvalbumin	Cd > Ca > Sr > Mg		Cave et al., 1979
Troponin C	Ca > Cd > Sr > Ba ~ Mg		Fuchs, 1971
Calmodulin	Ca ~ Cd > Sr > Ba ~ Mg		Chao et al., 1984

Table I also compares the Ca channel with other molecules in the relative affinity for various polyvalent cations. One distinguishing characteristic is the relative selectivity for Cd^{2+}. In binding Cd^{2+} in preference to Ca^{2+}, the Ca pore is at least qualitatively similar to EGTA and parvalbumin, and different from troponin and calmodulin. The overall conclusion from these comparisons is that the characteristics of the Ca channel fall within the range of behavior found for various Ca binding molecules. The idea that Ca channels and Ca binding proteins share a common ancestry remains a real possibility.

We thank E. W. McCleskey, R. L. Rosenberg, A. P. Fox, and J. A. Dani for helpful discussions, and S. C. Wong for technical assistance.

This work was supported by grants from the U.S. Public Health Service, Miles Pharmaceuticals, and Marion Laboratories.

Original version received 17 September 1985 and accepted version received 17 March 1986.

REFERENCES

Affolter, H., and R. Coronado. 1985. Agonists Bay-K8644 and CGP-28392 open calcium channels reconstituted from skeletal muscle transverse tubules. *Biophysical Journal.* 48:341–347.

Akaike, N., K. S. Lee, and A. M. Brown. 1979. The calcium current of *Helix* neuron. *Journal of General Physiology.* 71:509–531.

Almers, W., and E. W. McCleskey. 1984. Non-selective conductance in calcium channels in frog muscle: calcium selectivity in a single-file pore. *Journal of Physiology.* 353:585–608.

Almers, W., E. W. McCleskey, and P. T. Palade. 1984. A non-selective cation conductance in frog muscle membrane blocked by micromolar external calcium ions. *Journal of Physiology.* 353:565–583.

Almers, W., and P. T. Palade. 1981. Slow calcium and potassium currents across frog muscle membrane: measurement with a vaseline gap technique. *Journal of Physiology.* 312:159–176.

Anderson, M. 1983. Mn ions pass through calcium channels. A possible explanation. *Journal of General Physiology.* 81:805–827.

Armstrong, C. M. 1966. Time course of TEA^+-induced anomalous rectification in squid giant axons. *Journal of General Physiology.* 50:491–503.

Armstrong, C. M. 1969. Inactivation of the potassium conductance and related phenomena caused by quaternary ammonium ion injected in squid axons. *Journal of General Physiology.* 54:553–575.

Armstrong, C. M. 1975. Ionic pores, gates and gating currents. *Quarterly Review of Biophysics.* 7:179–210.

Bayley, P., P. Ahlstrom, S. R. Martin, and S. Forsen. 1984. The kinetics of calcium binding to calmodulin: Quin 2 and ANS stopped-flow fluorescence studies. *Biochemical and Biophysical Research Communications.* 120:185–191.

Byerly, L., P. B. Chase, and J. R. Stimers. 1985. Permeation and interaction of divalent cations in calcium channels of snail neurons. *Journal of General Physiology.* 85:491–518.

Cave, A., M.-F. Daures, J. Parello, A. Saint-Yves, and R. Sempere. 1979. NMR studies of primary and secondary sites of parvalbumins using the two paramagnetic probes Gd(III) and Mn(II). *Biochimie.* 61:755–765.

Chao, S.-H., Y. Suzuki, J. R. Zysk, and W. Y. Cheung. 1984. Activation of calmodulin by various metal cations as a function of ionic radius. *Molecular Pharmacology.* 26:75–82.

Colquhoun, D., and F. J. Sigworth. 1983. Fitting and statistical analysis of single-channel records. *In* Single Channel Recording. B. Sakmann and E. Neher, editors. Plenum Press, New York. 191–263.

Diebler, H., M. Eigen, G. Ilgenfritz, G. Maas, and R. Winkler. 1969. Kinetics and mechanism of reactions of main group metal ions with biological carriers. *Pure and Applied Chemistry.* 20:93–115.

Douglas, W. W. 1968. Stimulus-secretion coupling: the concept and clues from chromaffin and other cells. *British Journal of Pharmacology.* 34:451–474.

Edwards, C. 1982. The selectivity of ion channels in nerve and muscle. *Neuroscience.* 7:1335–1366.

Fuchs, F. 1971. Ion exchange properties of the calcium receptor site of troponin. *Biochimica et Biophysica Acta.* 245:2212–2229.

Fukuda, J., and K. Kawa. 1977. Permeation of manganese, cadmium, zinc, and beryllium through calcium channels of an insect muscle membrane. *Science.* 196:309–311.

Fukushima, Y. 1982. Blocking kinetics of the anomalous potassium rectifier of tunicate egg studied by single channel recording. *Journal of Physiology.* 331:311–331.

Fukushima, Y., and S. Hagiwara. 1985. Currents carried by monovalent cations through calcium channels in mouse neoplastic B lymphocytes. *Journal of Physiology.* 358:255–284.

Hagiwara, S. 1975. Ca-dependent action potential. *In* Membranes: A Series of Advances. G. Eisenman, editor. Marcel Dekker, New York. 3:359–381.

Hagiwara, S., and L. Byerly. 1981. Calcium channel. *Annual Review of Neuroscience.* 4:69–125.

Hagiwara, S., J. Fukuda, and D. C. Eaton. 1974. Membrane currents carried by Ca, Sr and Ba in barnacle muscle fiber during voltage clamp. *Journal of General Physiology.* 63:564–578.

Hagiwara, S., and K. Takahashi. 1967. Surface density of calcium ions and calcium spikes in the barnacle muscle fiber membrane. *Journal of General Physiology.* 50:583–601.

Hague, D. N. 1977. Dynamics of substitution at metal ions. *In* Chemical Relaxation in Molecular Biology. I. Pecht and R. Rigler, editors. Springer-Verlag, Berlin. 84–106.

Hesketh, T. R., G. A. Smith, J. P. Moore, M. V. Taylor, and J. C. Metcalfe. 1983. Free cytoplasmic calcium concentration and the mitogenic stimulation of lymphocytes. *Journal of Biological Chemistry.* 258:4876–4882.

Hess, P., J. B. Lansman, and R. W. Tsien. 1984. Different modes of Ca channel gating behavior favoured by dihydropyridine agonists and antagonists. *Nature.* 311:538–544.

Hess, P., J. B. Lansman, and R. W. Tsien. 1986. Calcium channel selectivity for divalent and monovalent cations. Voltage and concentration dependence of single channel current in ventricular heart cells. *Journal of General Physiology.* 88:293–319.

Hess, P., K. S. Lee, and R. W. Tsien. 1983. Ion-ion interactions in the calcium channel of single heart cells. *Biophysical Journal.* 41:293*a*. (Abstr.)

Hess, P., and R. W. Tsien. 1984. Mechanism of ion permeation through calcium channels. *Nature.* 309:453–456.

Hille, B. 1984. Ionic Channels of Excitable Membranes. Sinauer Associates, Sunderland, MA. 426 pp.

Hille, B., and W. Schwarz. 1978. Potassium channels as multi-ion, single-file pores. *Journal of General Physiology.* 72:409–442.

Kass, R. S., and R. W. Tsien. 1975. Multiple effects of calcium antagonists in cardiac Purkinje fibers. *Journal of General Physiology.* 66:169–192.

Katz, B. 1969. The Release of Neural Transmitter Substances. The Sherrington Lectures X. Liverpool University Press, Liverpool, U.K.

Kostyuk, P. G., and O. A. Krishtal. 1977. Effects of calcium and calcium-chelating agents on the inward and outward current in the membrane of mollusc neurones. *Journal of Physiology.* 270:569–580.

Kostyuk, P. G., S. L. Mironov, and Ya. M. Shuba. 1983. Two ion-selecting filters in the calcium channel of the somatic membrane of mollusc neurons. *Journal of Membrane Biology.* 76:83–93.

Lee, K. S., and R. W. Tsien. 1982. Reversal of current through calcium channels in dialyzed single heart cells. *Nature.* 297:498–501.

Lee, K. S., and R. W. Tsien. 1984. High selectivity of calcium channels in single ventricular heart cells of the guinea pig. *Journal of Physiology.* 354:253–272.

McCleskey, E. W., and W. Almers. 1985. The calcium channel in skeletal muscle is a large pore. *Proceedings of the National Academy of Sciences.* 82:7149–7153.

McCleskey, E. W., P. Hess, and R. W. Tsien. 1985. Interaction of organic cations with the cardiac Ca channel. *Journal of General Physiology.* 86:22*a*. (Abstr.)

Martell, A. E., and R. M. Smith. 1974. Critical Stability Constants. Vol. 1: Amino Acids. Plenum Press, New York and London.

Matsuda, H. 1986. Sodium conductance of calcium channels of guinea pig ventricular cells induced by removal of external calcium ions. *Pflügers Archiv.* In press.

Moore, W. J., and R. G. Pearson. 1981. Kinetics and Mechanism. 3rd ed. John Wiley & Sons, New York.

Muller, R. V., and A. Finkelstein. 1974. The electrostatic basis of Mg^{2+} inhibition of transmitter release. *Proceedings of the National Academy of Sciences.* 71:923–926.

Neher, E. 1983. The charge carried by single-channel currents of rat cultured muscle cells in the presence of local anaesthetics. *Journal of Physiology.* 339:663–678.

Neher, E., and J. H. Steinbach. 1978. Local anaesthetics transiently block currents through single acetylcholine-receptor channels. *Journal of Physiology.* 277:153–176.

Nelson, M. T. 1986. Interactions of divalent cations with single calcium channels from rat brain synaptosomes. *Journal of General Physiology.* 87:201–222.

Ochi, R. 1975. Manganese action potentials in mammalian cardiac muscle. *Experientia.* 31:1048–1049.

Potter, J. D., and J. D. Johnson. 1982. Troponin. *In* Calcium and Cell Function. W. Y. Cheung, editor. Academic Press, Inc., New York. 2:145–173.

Potter, J. D., J. D. Johnson, and F. Mandel. 1978. Fluorescence stopped flow measurements of Ca^{2+} and Mg^{2+} binding to parvalbumin. *Federation Proceedings.* 37:1608. (Abstr.)

Tsien, R. Y. 1980. New calcium indicators and buffers with high selectivity against magnesium and protons: design, synthesis, and properties of prototype structures. *Biochemistry.* 19:2396–2404.

Vereecke, J., and E. Carmeliet. 1971. Sr action potentials in cardiac Purkyne fibres. II. Dependence of the Sr conductance on the external Sr concentration and Sr-Ca antagonism. *Pflügers Archiv.* 322:73–82.

Yellen, G. 1984. Ionic permeation and blockage in Ca^{2+}-activated K^+ channels of bovine chromaffin cells. *Journal of General Physiology.* 84:157–186.